17

Electronic Biosensors Based on DNA Self-Assembled Monolayer on Gold Electrodes

Chen-Zhong Li[1,2], Yi-Tao Long[1,2], Todd Sutherland[1,2], Jeremy S. Lee[2], and Heinz-Bernhard Kraatz[1]
[1]Department of Chemistry, University of Saskatchewan, 110, Science Place, Saskatoon, SK, Canada [2]Department of Biochemistry, University of Saskatchewan, 107, Wiggins Road, Saskatoon, SK, Canada.
Current Address: Nanobiotechnology/Biosensor Group, Biotechnology Research Institute National Research Council Canada, 6100 Royalmount Avenue, Montreal, Quebec, Canada. e-mail:chenzong.Li@cnrc-nrc.gc.ca

Abstract: Information concerning the immobilization and hybridization of DNA on a surface is paramount to the development of DNA-based electronic biosensors. This study looks at recent investigations of DNA immobilized on gold surfaces using standard electrochemical techniques such as cyclic voltammetry (CV), potential step chronocoulometry and electrochemical impedance electrochemical impedance spectroscopy (EIS). The thiol-gold linkage is exploited for the immobilization of single- and double-stranded DNA onto gold electrodes. Two redox markers of opposite charge, ferricyanide and ruthenium hexaammine, respectively, are used to probe the environment in the vicinity of thiol-derivatized DNA electrodes. M-DNA is a form of DNA which allows the specific incorporation of certain metal ions into its helical structure under stringent conditions (i.e. low ionic strength and pH of 8.5). Single-stranded DNA monolayer and double strands DNA monolayer resistances were evaluated using EIS, respectively, and CV response were compared each other. The addition of Zn^{2+}, under M-DNA formation conditions, led to a dramatic enhancement of electrochemical response compared to B-DNA.

Key words: Electronic, biosensor, M-DNA, SAMs, electrochemistry.

1. Introduction

Methods for rapid single-nucleotide-polymorphisms (SNPs) detection are critical to the diagnosis of genetic and pathogenic diseases, tissue matching and forensic applications. The driving force behind DNA biosensor and gene chips development lies in the tremendous potential for obtaining sequence-

specific information in a faster, cheaper and more reliable manner compared to traditional hybridization assays.[1] Many techniques, including electrochemistry, have been developed or adapted for analyzing nucleic acids. Most detection systems utilize the hybridization of an immobilized target polynucleotide with oligonucleotide probes containing covalently linked reporter groups.[2] The fluorescence-based detection system is commonly used to perform on-chip SNP detection and gene expression. However, the fluorescence-based detection system is not favorable because of its requirement of complicated labeling process, expensive array chips and optical microarray scanners.[3,4]

An electrochemical DNA sensor or biosensor is another means of DNA detection and it has the advantages of sensitivity, rapid screening and easily implemented into conventional solid-state electronic devices. Therefore, the development of electrochemical transducer-based devices for determining nucleotide sequences and measuring DNA damage is an actively researched area. Recently, electrochemical devices have proven very useful for sequence-specific biosensing of DNA. Several groups[5-10] have reported SNP detection based on electrochemical techniques that use surface bound DNA, which do not contain covalently linked reporter molecules. Willner[11] uses a three component system involving tagged liposomes to amplify the Faradaic impedance signal. Barton[5] has reported SNP detection using several diffusible DNA intercalators. Cyclic voltammagrams clearly show an enhanced current response for duplex DNA and a suppressed response for DNA that contains one mismatched base pair. In a similar system, Takenaka[10] has employed ferrocenyl naphthalene diimide (FND) as an intercalator. Their results show an enhanced current for complementary DNA using differential pulse voltammetry (DPV). The basis of this method lies in FND's ability to bind matched DNA. A mismatch in sequence has the effect of creating disorder in the helical structure and as a result, FND does not bind and signal intensity is attenuated.

Information concerning the immobilization of single-stranded DNA (ss-DNA) and duplex DNA (ds-DNA) on a surface is paramount to the development of DNA-based electronic biosensors. Electrochemical detection of DNA immobilization and hybridization usually involves monitoring a current response under controlled potential conditions. Self-assembly of DNA monolayer based on the formation of a gold-thiolate bond is an important method for preparing stable, closely packed monolayers with well-defined structures.[12,13] Although hybridization efficiencies of both ss- and ds-DNA derivatized gold surfaces have been characterized by several groups,[13,14] the electrochemical properties of M-DNA self-assembled monolayers (SAMs) on gold surfaces have never been examined. M-DNA is a form of duplex DNA with divalent metal ions such as Zn^{2+} that forms at basic pH (pH 8.5) and low ionic strength ($\mu = 0.05$). The electrochemical signal can be enhanced due to M-DNA formation on ds-DNA modified electrode surface.[15-17] Until a crystal structure is available, the proposed structure of M-DNA has the metal ions replace the imino protons of guanine and thymine at every base pair (Figure 17-1). Addition of EDTA will sequester the metal ions and convert

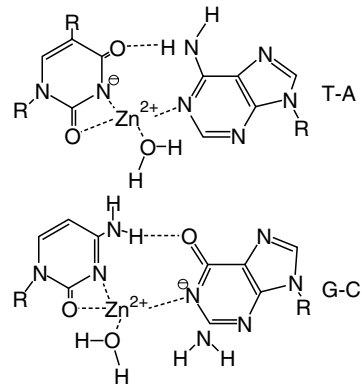

FIGURE 17.1. Possible base-pairing schemes for M-DNA.

the M-DNA back to normal DNA (B-DNA). Alternatively, a decrease in pH will also cause the M-DNA structure to return to B-DNA.

Preliminary evidence demonstrated that M-DNA is an efficient conductor of electrons over distances as long as 500 base-pairs and possibly as long as several microns.[18,19] The enhanced conductivity of M-DNA should allow a greater signal to background current ratio and thus make it more sensitive to perturbations caused by hybridization than B-DNA[15,16] (Figure 17.2).

In this paper a scheme for the voltammetric study of ss-DNA and ds-DNA self assembled monolayers (SAMs) on gold electrodes is presented. Gold surfaces were modified by 20-base-pair 5′-thiol-linked DNA oligonucleotides through the S-Au bond. The electrochemical properties of bare electrode, ss-DNA and ds-DNA modified electrodes were investigated using two redox

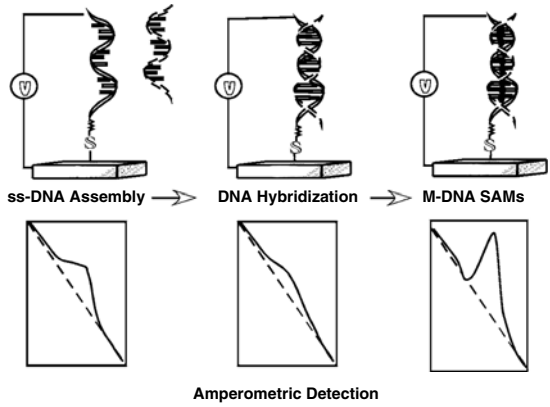

FIGURE 17.2. Schematic representation of the electronic DNA sensor for electrochemical detection for DNA hybridization.

markers of opposite charge, ferricyanide and ruthenium hexaammine, respectively. The mediated effect of metal intercalated within ds-DNA on the electron transfer was described to enhance the sensitivity for DNA hybridization detection. The major advantage of these techniques is that the target DNA strand need not be labeled in advance.

2. Materials and Methods

2.1 General

$Ru(NH_3)_6Cl_3$, $Ru(NH_3)_6Cl_4$, $K_3Fe(CN)_6$ and $K_4Fe(CN)_6$ were purchased from Aldrich and used without further purification. $Zn(ClO_4)_2$, $Mg(ClO_4)_2$ and Tris-ClO_4 were purchased from Fluka. Deionized water (18 MΩzcm resistivity) from a Millipore Milli-Q system was used throughout this work.

2.2 Oligonucleotide Synthesis

Three oligonucleotides were purchased from the Plant Biotechnology Institute-National Research Council (PBI-NRC, Saskatoon) with the following base sequences:

1 SS-5′-GTCACGATGGCCCAGTAGTT-3′
2 5′-AACTACTGGGCCATCGTGAC-3′ (complement of **1**)
3 5′-GTCACGATGGCCCAGTAGTT-3′ (noncomplementary strand containing the same sequence as **1** but lacks the SS 5′ linker)

Note: SS 5′ refers to HO_3PO-$(CH_2)_6$-SS-$(CH_2)_6$-OH

The oligonucleotides were synthesized by standard phosphoramidite chemistry[20] using a fully automated DNA synthesizer then purified by two-step reversed-phase HPLC and characterized by MALDI-TOF mass spectrometry.

2.3 X-Ray Photoelectron Spectroscopy (XPS)

A Leybold MAX200 photoelectron spectrometer equipped with an Al-K_α radiation source (1486.6 eV) was used to collect photo emission spectra. The base pressure during measurements was maintained at less than 10^{-9} mbar in the analysis chamber. The take-off angle was 60°. The routine instrument calibration standard was the Au $4f_{7/2}$ peak (binding energy 84.0 eV).

2.4 Electrochemical Measurements

A potentiostat/galvanostat (EG&G model 283) and Impedance frequency analyzer (EG&G model 1025) connected to a PC running Power Suite (Princeton Applied Research) was used for Impedance spectroscopy measurements. A BAS Model CV-50W potentiostat was used for

underpotential deposition (UPD), chronoamperometry and cyclic voltammetry experiments.

2.5 Electrode Characterization and Pretreatment

Gold disk electrodes (Bioanalytical Systems, 1.6 mm diameter, ca. 0.02 cm^2 geometrical area, roughness coefficients between 1.2 and 1.4) were used for the electrochemical measurement. Before modification, the electrode surface was cleaned by electrochemical sweeping in 0.1 M H_2SO_4 from 0 to 1.4 V, then rinsed with water, and ultrasonicated for 5 minutes in fresh piranha solution (30% H_2O_2, 70% H_2SO_4). WARNING: PIRANHA SOLUTION REACTS VIOLENTLY WITH ORGANIC SOLVENTS. The electrode was then sonicated by distilled and degassed ethanol, and finally rinsed with Milli-Q water. A cyclic voltammagram recorded in 0.1 M H_2SO_4 (scan rate 100 $mV.s^{-1}$) was used to determine the active area of the electrode surface. The real electrode surface area and roughness factor were obtained by integration of the gold oxide reduction peak.[21,22]

2.6 Preparation of DNA SAMs

Duplex DNA modified surfaces were prepared by initially hybridizing the two complementary strands in the absence of a Au surface in a hybridization buffer (100 mM Tris-ClO_4, 100 mM $NaClO_4$, pH 7.5) for 24 hours at a DNA concentration of 0.2 mM. The Au electrode was then incubated in the same hybridization buffer for three days at room temperature. Upon completion of monolayer formation, the electrodes were washed repeatedly with (50 mM Tris-ClO_4, pH 8.6) for five minutes. The incubation was allowed to continue for one additional day at which time it was rinsed three times with buffer (50 mM Tris-ClO_4, pH 8.6). The electrode surface coverage of ds-DNA was quantified to be over 90% by the underpotential deposition (UPD) of Cu.[15,23,24]

The ss-DNA of **1** modified surfaces were formed by dehybridization of ds-DNA from the surface by immersing the ds-DNA modified surface in a water/EtOH solution for 5 minutes at 37 ˚C. Rehybridization of **1** and **2** was performed at 37 ˚C for 60 minutes in SSC buffer (300 mM NaCl/30 mM Sodium Citrate, pH 7.0). The concentration of complementary strand **2** or noncomplementary strand **3** was 0.1 mM. Each sample was rinsed thoroughly with an excess volume of 100 mM Tris-ClO_4 buffer and dried under a stream of argon prior to characterization. This method of producing a ss-DNA modified surface provide a more reproducible surface compared to straight incubating with ss oligonucleotide **1**. In addition, this methodology will limit the amount of ss-DNA that can form bonds from the exposed base pairs' nitrogen to the gold surface[12].

The ds-DNA monolayer was converted into the M-DNA monolayer by exposure of the monolayer to a solution of 0.3 mM $Zn(ClO_4)_2$ in 20 mM Tris-ClO_4 buffer (pH 8.6) for at least two hours.

2.7 Electrochemical Measurements

A normal three-electrode configuration consisting of the modified Au-electrode working electrode, a Ag/AgCl/3M NaCl reference electrode (BAS) and a platinum wire auxiliary electrode. The cell was enclosed in a grounded Faraday cage. A glass-frit salt-bridged reference electrode was used to limiting Cl^- ion leakage for the normal Ag/AgCl reference electrode to the measurement system. The open-circuit, or rest potential, of the system was measured prior to all electrochemical experiments in order to prevent sudden potential related changes in the SAM. All electrochemical experiments were started from this rest potential. UPD experiments were carried out in 1 mM $Cu(ClO_4)_2$ in 0.1 M $HClO_4$ at a scan rate of 10 mV˜s^{-1}, starting at 500 mV (vs. Ag/AgCl), cathodic scanning to 50 mV followed by an anodic sweep to 600 mV. Impedance was measured at the potential of 250 mV vs. Ag/AgCl, to which a sinusoidal potential modulation of ±5 mV was superimposed. The frequencies used for impedance measurements ranged from 100 kHz to 100 mHz. The impedance data for the bare gold electrode, ss-DNA, ds-DNA and M-DNA modified gold electrode were analyzed using the ZSimpWin software (Princeton Applied Research). In all impedance spectra, symbols represent the experimental data, and the solid lines represent the fitted curves.

3. Results and Discussion

As previously described[12,25], many thiol-derivatized ss-DNA molecules may interact with the gold surface non-specifically. Non-specific interaction is defined as physisorption, such as nitrogen atom or polar side chain interactions, as opposed to chemisorption herein defined as covalent bond formation between Au-S. However, for ds-DNA, because nucleic acid bases are directed toward one another, the non-specific interactions with the Au surface will be very weak and multilayers can simply be removed with buffer rinsing.[26] Thus, in the ds-DNA case, the final structure is most likely to arrive from specific interaction through the covalent Au-S bond formation. A ds-DNA SAM of **1** and **2** results in a mixed monolayer gold, with the ds-DNA-S adjacent to a hydroxylalkyl-S group (Figure 17.3). This arrangement should reduce the efficiency of non-specific interaction of ds-DNA with the gold surface. As previously reported by Tarlov and co-workers, a competitive adsorption step using methylene thiol spacer was deemed necessary to prepare a ss-DNA monolayer with high hybridization ability and few non-specifically adsorbed ss-DNA molecules.[12,13] However, this procedure led to a displacement of some covalently attached DNA-thiolate by the alkylthiol in a well-understood thiol exchange reaction and decreased the surface density of ss-DNA strands.[25,26] In the present study, to prepare ss-DNA modified electrode surface, unlike previous studies, ss-DNA was formed by first adsorbing duplex DNA and then dehybridizing the duplex by immersion in water and

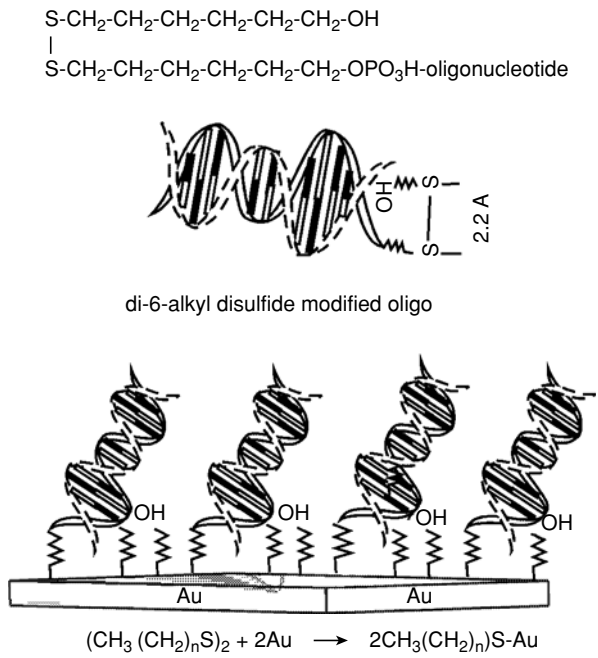

FIGURE 17.3. Schematic representation of proposed model of the mixed SAMs by dialkyl disulfide ds-DNA on gold surface.

EtOH. The advantages of this methodology are that the loss of covalently attached ss-DNA is low and non-specific binding of DNA is minimized. The ss-DNA, **1**, covered surface will be regenerated and is capable of hybridizing with complementary DNA repeatedly[12], though the chemical or thermally-induced dehybridization of ds-DNA on surface may effect the ability of DNA rehybridization[13] on electrode surface. An important parameter in this methodology is the efficiency[13,27,28] with which the original ds-DNA surface can become dehybridized.

3.1 Analysis of ds-DNA Modified Electrode Surface

Modification of gold surfaces with DNA-hydroxyalkyl disulfide terminated DNA duplexes were confirmed by UPD and XPS experiments. Underpotential deposition of copper has been proved to be a useful tool to evaluate the area of exposed gold remaining after monolayer formation.[24,29] Figure 17.4 shows typical cyclic voltammograms (CVs) of a bare Au electrode and the ds-DNA modified electrode taken in 1.0 mM $Cu(ClO_4)_2$, 50 mM $HClO_4$ aqueous solution at a scan rate of 10 mV s^{-1}. As expected, the Cu UPD on the bare electrode produced a pair of well-separated broad peaks.

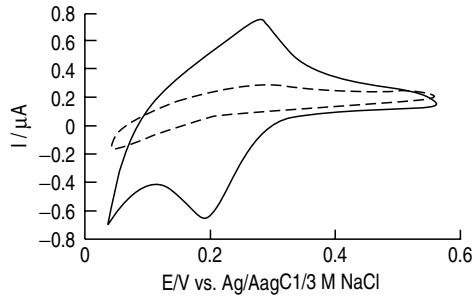

FIGURE 17.4. Under potential deposition of copper on bare (—) and ds-DNA modified gold electrode (-----); 1 mM $Cu(ClO_4)_2$ + 0.05 M $HClO_4$, scan rate was 10 $mV^{-}s^{-1}$. The gold electrode area was 0.02 cm^2.

During the negative-going scan the Cu is deposited on all accessible Au surface and the the anodic peak corresponds to the stripping wave as Cu is oxidized from the surface.[30,31] In contrast to the bare gold, UPD of Cu was strongly suppressed by a ds-DNA monolayer. Although, a small Cu-UPD stripping peak at 0.310 V, due to Cu/Cu^{2+}, in present results show that the ds-DNA/alkyl SAMs does not completely block the Au electrode even after 4 days of incubation. The integration of the stripping wave for the modified electrode was only 5% of the bare electrode. This indicated that the ds-DNA/6-hydroxylalkyl mixed SAMs can act as an effective barrier for electron transfer even though there are still a few defects in the ds-DNA blocking layer.[15] Note that since the amount of charge calculated from CV often contains contributions from co-adsorbed electrolyte anions to some extent, it is not always correct to determine the actual exposed electrode area from CVs alone.[30,32]

The gold surface was also analyzed by X-ray photoelectron spectroscopy (XPS). As shown in Figure 17.5, the intensity of the Au4f peaks decrease upon attachment of the DNA as expected for a modified surface.[33] The monolayers presence is confirmed by the following new peaks which are absent in bare Au spectra: S2p (162.4 eV), P2p (133 eV) and N1s (400 eV). Furthermore, the value of 162.4 eV for the S2p peak is in good agreement with previous reports for alkylthiol SAMs indicating the specific formation of the Au-S bond of ds-DNA to the gold surface.[34] Film thickness was estimated based on the exponential attenuation of the Au4f signal and calculated to be 45 Å.[35] A 20 base-pair duplex is expected to have a length of about 70 Å so a measured thickness of 45 Å is consistent with the fact that the DNA helices are packed at an angle with respect to the surface.[16] Hence, the morphology of the ds-DNA modified surface appears to involve a densely packed array of duplexes.

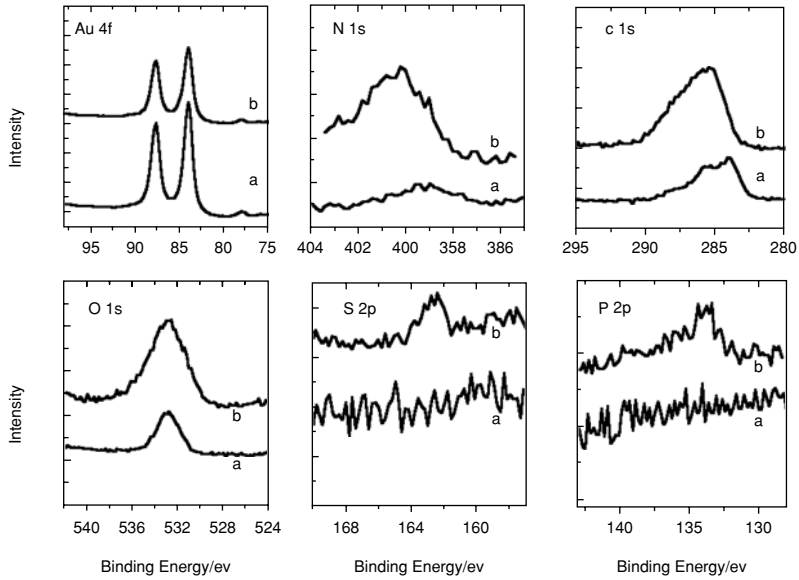

FIGURE 17.5. XPS spectra of (a) bare gold, (b) 20 base-pair thiol-derivatized ds-DNA assembled on gold.

3.2 *Electrochemical Impedance Spectroscopy (EIS) for DNA Dehybridization and Rehybridization on Surface*

EIS is an effective method to probe the interfacial properties of surface-modified electrodes.[36] EIS data analysis requires modeling the electrode kinetics with an equivalent circuit consisting of electrical components. The general electronic equivalent scheme (Figure 17.6a) for a alkanethiol monolayers-modified electrode is usually described[37] on the basis of the model developed by Randles and Ershler.[38] This equivalent circuit is that of the solution Ohmic resistance R_s in series with a parallel network of the double layer capacitance C_{dl} and the interfacical electron-transfer resistance R_{ct}. Z_w is the

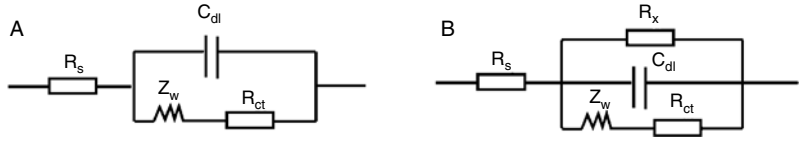

FIGURE 17.6. (a) Standard Randles and Ershler model circuits used to fit the bare electrode; (b) Compartmentalized equivalent circuit used to model DNA modified electrodes. The values of each element in circuits calculated by the computer fitting of the experiment spectra with these circuits are collected in Table 17.1.

Warburg impedance resulting form the diffusion of ions form the bulk electrolyte to the electrode interface. The complex impedance can be presented as the sum of the real, $Z_{re}(\omega)$, and imaginary, $Z_{im}(\omega)$, components originating mainly from the resistance and capacitance of the cell, respectively. The negatively charged $Fe(CN)_6^{3-}/Fe(CN)_6^{4-}$ (1:1 mixture) was used as the redox probe to elucidate the electrical properties of ds-DNA, ss-DNA and rehybridized ds-DNA monolayer by EIS. Figure 17.7a shows a Nyquist plot of the raw data (symbols) for the bare gold electrode and the theoretically best fit curves (solid lines) resulting from the Randles circuit of Figure 17.6.

The semicircle portion, measured at higher frequencies, corresponds to direct electron transfer limited process, whereas the linear portion, observed at lower frequencies, represents the diffusion controlled electron transfer process. In the case of ds-DNA modified electrode, the experimental data in the low frequency region was not adequately fit using Randles circuit model (Figure 17.6a), an additional interfacial resistance, R_x, was added in parallel to the equivalent circuit (Figure 17.6b), termed the modified Randles circuit, that corresponds to electron transfer through the DNA. As shown in Figure 17.6b, the modified circuit gives an excellent fit to the experimental data in all frequency regions for a DNA modified surface. Table 17-1 summarizes the fitting results. ds-DNA shows a larger interfacial electron transfer resistance than that of bare gold indicating that the redox probe is electrostatically repelled by the negatively charged DNA monolayer that is bound to the electrode. After the dehybridization treatment, a significant decrease in R_x and

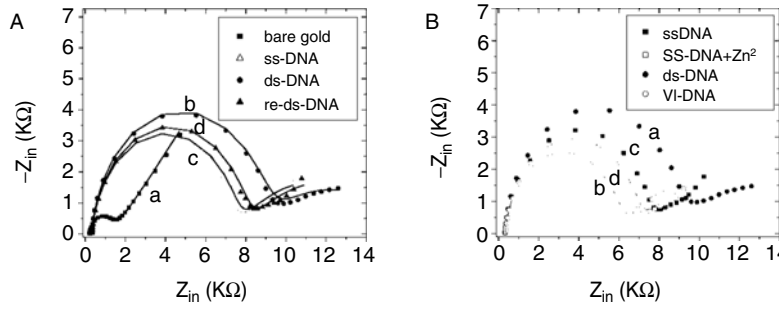

FIGURE 17.7. (A) Nyquist plot (Z_{im} vs.Z_{re}) for the Faradaic impedance measurements at (a) a bare Au electrode, (b) a ds-DNA modified electrode, (c) ss-DNA modified electrode upon de-hybridization treatment of (b), (d) re-hybridized ds-DNA modified electrode. (B) Nyquist plot for the Faradaic impedance measurements at (a) ds-DNA modified electrode, (b) M-DNA formed electrode upon incubating (a) in the buffer solution containing 0.3 mM $Zn(ClO_4)_2$ for two hours. (c) ss-DNA modified electrode, (d) ss-DNA modified electrode (c) treated as the same condition as (b). The measurements were performed in the presence of 5 mM $Fe(CN)_6^{3-/4-}$ in 20 mM Tris-ClO_4 and 20 mM $NaClO_4$ solution, upon application of a biasing potential of 0.25 V vs. Ag/AgCl. Solid Lines correspond to the theoretical fit of the experiment data.

TABLE 17.1. Comparison of the resistance and capacitance values derived from the EIS of the bare electrode and DNA modified electrodes in the presence of 5 mM $Fe(CN)_6^{3-/4-}$ as redox probe upon fitting the experiment data with the equivalent circuits shown in Figure 17.6

Element	Bare Au†	ds-DNA‡	rehybridized ds-DNA‡	M-DNA‡	ss-DNA‡	ss-DNA with Zn^{2+}‡
R_s/Ω	302	320	334	338	337	314
R_X/Ω		16200	15600	12900	15300	14500
$C/\mu F$	2.6	0.29	0.29	0.285	0.28	0.31
R_{ct}/Ω	1230	18800	14900	10000	13500	12100
$W/10^{-5}\Omega s^{-1/2}$	27	3.9	6.6	8.2	7.5	7.9

†Values calculated using Randles circuit (Figure 17.6a).
‡Values calculated using modified Randles circuit (Figure 17.6b).

R_{ct} was observed. The decrease in the electron-transfer resistance upon dehybridization of ds-DNA is consistent with the idea that the density of the negatively charged phosphates is decreased, which permits penetration of the negatively charged redox marker. Also, an increase in the number or area of defect sites created from the dehybridization cannot be discounted as a plausible explanation for the decrease in R_X and R_{ct}. The rehybridization behavior of surface-immobilized ss-DNA was also determined by impedance spectroscopy. Relatively long hybridization times, 60 minutes, and high salt concentrations, SSC buffer, were used to maximize duplex yield. It was clear form the impedance data that both R_X and R_{ct} increased indicating that complementary strand **2** hybridized with the surface-bound **1**. As a control, rehybridization experiments with noncomplementary strand **3**, showed no increase in the measured electron-transfer resistances. Note that the R_X and R_{ct} for rehybridized surface are still smaller than that of the original ds-DNA modified surface. There are two reasons to be considered. First, the rehybridization efficiency of the ss-DNA attached on gold surface is less than 100% [13], leading to a mixed monolayer that consists of both ss-DNA and ds-DNA. Second, the chemical dehybridization process may result in desorption of ss- or ds-DNA from the surface, resulting in an increase in the amount of surface accessible gold surface.

M-DNA is a novel conformation of duplex DNA in which metal ions, such as Zn^{2+}, are inserted into the helix. M-DNA can also be formed on a surface-immobilized ds-DNA strand under similar condition as solution, except taking much more time. Upon addition of Zn^{2+} to a 20-mer of B-DNA modified gold electrode at pH 8.7 and incubating for 2 hours, the impedance spectrum changed. The differences result in a distinctive pattern with a reduction in Z_{im} and Z_{re} at both high and low frequencies (Figure 17-7b). It is clear that there are significant decreases in R_X and R_{ct} upon addition of Zn^{2+} to ds-DNA modified electrode, which are not found upon addition of Zn^{2+} to ss-DNA modified electrode.[16] The decrease of R_X and R_{ct} following M-DNA formation can be explained by an enhanced rate of electron transfer through

the M-DNA monolayer. The fitting results for all modified surfaces are shown in Table 17.1.

3.3 Cyclic Voltammetry and Chronocoulometry at DNA-Modified Electrodes

Generally, two electrochemical systems are commonly used to probe the electrochemical properties of DNA SAMs. One system utilizes an electroactive SAM whereby the redox probe is covalently attached to molecules forming on the DNA monolayer.[17,39,40] The other system, the electron transfer occurs between the gold electrode surface and a redox probe that freely diffuses in solution. The present study focuses on the latter system using an anionic $Fe(CN)_6^{3-/4-}$ or a cationic $Ru(NH_3)_6^{3+/4+}$ redox system.

The voltammagram for these two redox markers at a bare gold electrode is given in Figure 17.8 and Figure 17.9, respectively. Both exhibit a reversible or quasi-reversible, diffusion-limited, one-electron redox process in aqueous buffer solution. A comparison of ss-DNA, ds-DNA and bare gold cyclic voltammagrams with $Fe(CN)_6^{3-}$ is shown in Figure 17.8. Two features of the CV provide evidence that the modified surface is blocked to an anionic redox probe. First, the large peak-to-peak separation (ΔE_p) of both ss- and ds-DNA compared to that of the bare Au and second, the decrease in peak currents (only 5% –15% compared to bare gold). The blocking characteristics of a DNA modified surface is explained by the physical barrier presented to the redox probe. If the redox probe is unable to get close to the electrode then the probability that electron transfer will occur falls off dramatically. In the case of DNA, the monolayer is also negatively charged, due to the phosphate

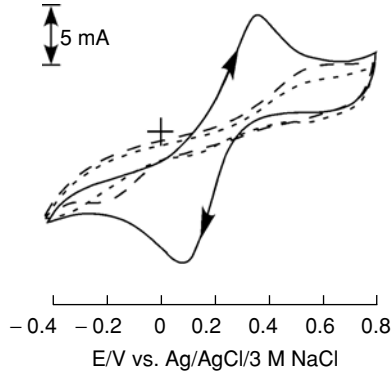

FIGURE 17.8. Cyclic voltammagrams for 2.5 mM $Fe(CN)_6^{3-/4-}$ in 20 mM Tris-ClO_4 buffer (pH 8.6) at a bare electrode (—), a ds-DNA modified electrode (----)and a ss-DNA modified electrode (— — —) upon de-hybridization of duplex DNA modified electrode. The sweep rate was 100 mV˜s^{-1}.

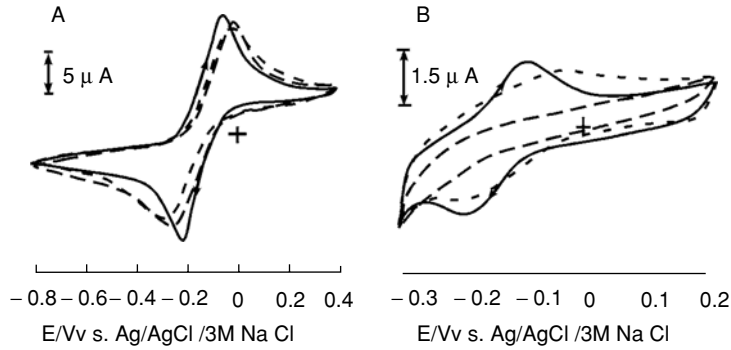

FIGURE 17.9. (A) Cyclic voltammograms for 5.0 mM $Ru(NH_3)^{3+/2+}$ in 20 mM Tris-ClO_4 buffer (pH 8.6) at a bare electrode (—), a ds-DNA modified electrodes (— — —) and a ss-DNA modified electrode (------). (B) Cyclic voltammagrams at a ds-DNA modified electrode (—), a ss-DNA modified electrode (------) in blank buffer (20 mM Tris-ClO_4, pH 8.6) after incubation treatment in 5 mM $Ru(NH_3)^{3+/2+}$ solution, and a ds-DNA modified electrode in blank buffer after incubation treatment (— — —) in 2.5 mM $Fe(CN)_6^{3-/4-}$ solution. The sweep rate was 100 $mV\tilde{s}^{-1}$.

backbone, and this will electrostatically repel an anionic redox probe. In addition, note the small difference in blocking behaviors for redox probes between ss- and ds-DNA modified gold surfaces. As expected, Figure 17.8 shows the redox peak current for ss-DNA monolayer is slightly larger relative to that of ds-DNA monolayer. This is explained by a decrease in negative charge density on the SAM. The slightly lower negative charge density for ss-DNA manifests in a slightly larger peak current.

In contrast, the positively charged $Ru(NH_3)_6^{3+/4+}$ redox probe is not effectively blocked by the DNA monolayer. Figure 17.9A shows the CVs for ss-DNA modified, ds-DNA modified and bare gold electrodes. The peak separation for bare Au is 0.17 V, whereas, a ds-DNA modified electrode shows only a modest increase to 0.20 V. Assuming the coverage of the Au electrode is the same as in the anionic redox probe scenario, this suggests that cationic species is attracted by the negatively charged DNA backbone. The formation of electrostatic bonds along the phosphate backbone allows the cationic redox probe to approach the electrode surface and give rise to reversible electrochemical behavior similar as that of a bare electrode. Additional support for the electrostatic interaction of DNA SAMs with cationic species is evident from Figure 17.9B. Following extensive rinsing, the $Ru(NH_3)_6^{3+/4+}$ exposed ss- or ds-DNA modified electrodes still indicate a large amount redox probe remains bound to the monolayer. This behavior was not observed for the anionic redox probe.

Conversion of ds-DNA to an M-DNA monolayer was achieved by exposing the electrode to 20 mM Tris buffer (pH 8.5) containing 0.3 mM $Zn(ClO_4)_2$ for 2 hours. Figure 17.10A shows the electrochemical signal due to the

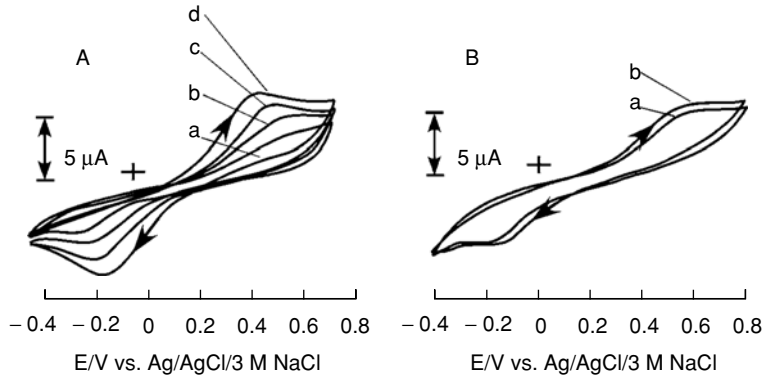

FIGURE 17.10. Cyclic voltammagrams corresponding to the time-dependent formation of M-DNA on a gold surface from (A) ds-DNA modified electrode achieved by re-hybridization of **1** with **2**: (a) 0 minutes, (b) 20 minutes, (c) 50 minutes and (d) 120 minutes. (B) ss-DNA modified electrode treated at the same hybridization condition as (A) except with non-complementary strand **3**: (a) 0 minute, (b) 120 minutes. Data were recorded by the condition outlined in Figure 17-8 with the addition of 0.3 mM $Zn(ClO_4)_2$.

$Fe(CN)_6^{3-/4-}$ is significantly increased during the 2 hour incubation time with Zn^{2+}. The integrated area of the M-DNA peak after 2 hours is at 80% of the bare Au integrated peak area. The peak area remains unchanged for incubation times longer than 2 hours. Conversely, with ss-DNA, the peak area only increases slightly over the same incubation time (Figure 17.10B). The electron transfer kinetics have become faster due to M-DNA formation as is evident from the increase in the peak current and in the decrease of peak separation. Two ss-DNA modified electrode samples were then re-exposed to either the complementary strand **2** or the noncomplementary strand **3**. Hybridization occurred with complementary strand **2**, as expected, and resulted in a slight change in the redox peak current of $Fe(CN)_6^{3-/4-}$. Furthermore, a significant change in the redox peak current was observed following M-DNA formation only when the complementary target **2** was hybridized with the surface-bound ss-DNA (Figure 17.11). Thus, the mediated effect of metal intercalated within M-DNA on the electron transfer provides a powerful tool to enhance differentiation of the electrochemical signal between complementary and non-complementary, and allows electrical detection of the DNA hybridization on a surface.

A charge integration technique, chronoamperometry, has been reported to be a practical charge transport-based technique to electrically characterize SNPs[7,41,42] or to quantitatively determine the surface density of immobilized DNA. This methodology, based on measuring the charge transport through

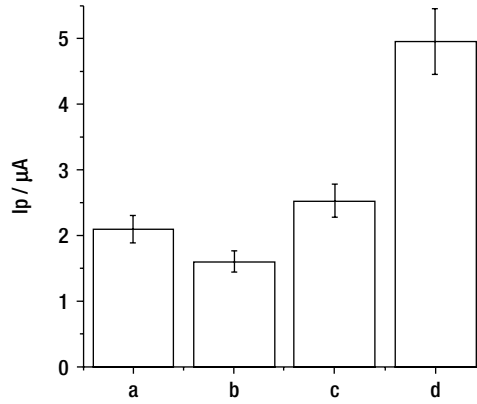

FIGURE 17.11. Sensitivity profile for electrochemical detection of DNA hybridization on an electrode surface. The values represent the redox peak current of $Fe(CN)_6^{3-/4-}$ at different electrodes. (a) **1** modified electrode with non-complement strand **3**. (b) **1** modified electrode with complement strand **2**. (c) **1** modified electrode with non-complement strand **3** under M-DNA forming conditions. (d) **1** modified electrode with complement strand **2** under M-DNA forming conditions.

DNA films, was employed on the same set of redox systems under identical experimental conditions. The initial potential started at 200 mV vs. Ag/AgCl where no electrolysis of ferricyanide occurs. Comparison of the charge passed at ss-DNA, ds-DNA and M-DNA modified electrode is shown in Figure 17.12. During a single step of 12 s to –350 mV, where essentially all the $Fe(CN)_6^{3-}$ is reduced to $Fe(CN)_6^{4-}$. The amount of charge passed on

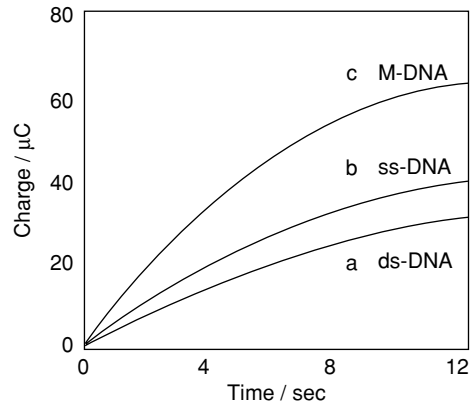

FIGURE 17.12. Chronocoulometric transients at –350 mV of 5 mM ferricyanide in 20 mM Tris-ClO_4 buffer (pH 8.6) at (a) ds-DNA modified electrode (b) ss-DNA modified electrode and (c) M-DNA modified electrode.

M-DNA modified electrodes is significantly larger than that of either ss-DNA or ds-DNA modified electrodes. These experiment confirmed the results of CV, that M-DNA is a better electron transfer mediator than both ss- and ds-DNA.

4. Conclusions

The present study has addressed the development of electronic DNA sensors by monitoring changes in the electric properties of ss-, ds- and M-DNA monolayers on gold electrode surface. We have characterized thiol-derivatized DNA attached to gold via a sulfur-gold linkage using XPS, and electrochemical experiments. These results indicate that a ds-DNA monolayer with high surface coverage can be prepared using ds-DNA-hydroxylalkyl disulfide and the SAM is capable of hybridization with complementary DNA after dehybridizaiton treatment. Specifically, our immobilization method avoids the indiscriminate replacement of the DNA probes through competitive alkanethiol replacement. Furthermore, a direct, label-free, electriconic detection of DNA hybridization has been accomplished by monitoring changes in the electrochemical signal at DNA-modified electrodes by EIS, CV and chronoamperometry methods. Our results highlight the sensitivity, based on better conductivity properties of M-DNA, of the hybridization sensing process. Therefore, M-DNA may find widespread applications in nanoelectronics or biosensing since a direct electrical readout of hybridization or DNA binding is now possible.

Acknowledgements. The authors wish to thank CIHR, NSERC and UMDI for financial support, H-B. K. holds a Canadian Research Chair in biomaterials and J. S. L. is supported by a Senior Investigators Award from the Regional Partnership Program of CIHR. The authors also thank Dr. Herrwerth, the University of Heidelberg, Germany, for performing the XPS measurements.

References

1. Razin, S. *Mol. Cell. Probes* **1994**, *8*, 497–511.
2. Hames, B. D.; Higgins, S. J. *Gene Probes 1*; IRL Press: New York, 1995.
3. Fodor, S. P. A.; Rava, R. P.; Huang, X. C.; Pease, A. C.; Holmes, C. P.; Adams, C. L. *Nature* **1993**, *364*, 555.
4. Schena, M.; Shalon, D.; Davis, R. W.; Brown, P. O. *Science* **1995**, *270*, 467.
5. Boon, E. M.; Salas, J. E.; Barton, J. K. *Nat. Biotechnol*. **2002**, *20*, 282–286.
6. Hashimoto, K.; Ishimori, Y. *Lab on a Chip* **2001**, *1*, 61–63.
7. Kelley, S. O.; Boon, E. M.; Barton, J. K.; Jackson, N. M.; Hill, M. G. *Nucleic Acids Res*. **1999**, *27*, 4830–4837.
8. Lee, T. M. H.; Hsing, I. M. *Anal. Chem*. **2002**, *74*, 5057–5062.
9. Lioubashevski, O.; Patolsky, F.; Willner, I. *Langmuir* **2001**, *17*, 5134–5136.

10. Yamashita, K.; Takagi, M.; Kondo, H.; Takenaka, S. *Anal. Biochem*. **2002**, *306*, 188–196.
11. Patolsky, F.; Lichtenstein, A.; Willner, I. *J. Am. Chem. Soc*. **2001**, *123*, 5194–5205.
12. Herne, T. M.; Tarlov, M. *J. J. Am. Chem. Soc*. **1997**, *119*, 8916–8920.
13. Peterlinz, K. A.; Georgiadis, R. M.; Herne, T. M.; Tarlov, M. J. *J. Am. Chem. Soc*. **1997**, *119*, 3401–3402.
14. Georgiadis, R. M.; Peterlinz, K. A.; Peterson, A. W. *J. Am. Chem. Soc*. **2000**, *122*, 3166–3173.
15. Li, C-Z.; Long, Y-T.; Kraatz, H.-B.; Lee, J. S. *J. Phys. Chem. B* **2003**, *107,* 2291-2296.
16. Long, Y-T.; Li, C-Z.; Kraatz, H.-B.; Lee, J. S. *Biophys. J*. **2003**, *84,* 3218-3225.
17. Wetting, S. D.; Li, C-Z.; Long, Y-T.; Kraatz, H.-B.; Lee, J. S. *Anal. Sci.* **2003**, *19,* 23-26.
18. Aich, P.; Labiuk, S. L.; Tari, L. W.; Delbaera, L. J. T.; Roesler, W. J.; Falk, K. J.; Steer, R. P.; Lee, J. S. *J. Mol. Biol*. **1999**, *294*, 477–485.
19. Lee, J. S.; Latimer, L. J. P.; Reid, R. S. *Biochem. Cell Biol*. **1993**, *71 (3-4)*, 162–168.
20. Wincoff, F.; Direnzo, A.; Shaffer, C.; Sweedler, D.; Gonzalez, C.; Scarinje, S.; Usman, N. *Nucleic Acids Res*. **1995**, *25*, 2677–2684.
21. Woods, R.; Bard, A. J.; Dekker, M. *Electroanalytical Chemistry*; 1 ed.: New York, 1980.
22. Hallmark, V. M.; Chiang, S.; Rabolt, J. F.; Swalen, J. D. *Phys. Rev. Lett*. **1987**, *59*, 2879.
23. Eliadis, E. D.; Nuzzo, R. G.; Gewirth, A. A.; Alkire, R. C. *J. Electrochem. Soc*., **1997**, *144*, 96–105.
24. Sun, L.; Crooks, R. M. *J. Electrochem. Soc*., **1991**, *138*, L23–L25.
25. Steel, A. B.; Levicky, R. L.; Herne, T. M.; Tarlov, M. J. *Biophys. J*. **2000**, *79*, 975–981.
26. Yang, M.; Yau, H. C. M.; Chan, H. L. *Langmuir* **1998**, *14*, 6121–6129.
27. Kertesz, V.; Whittemore, N. A.; Inanati, G. B.; Manoharan, M.; Cook, P. D.; Baker, D. C.; Chambers, J. Q. *Electroanalysis* **2000**, *12*, 889–894.
28. Kertesz, V.; Whittemore, N. A.; Chambers, J. Q.; McKinney, M. S.; Baker, D. C. *J. Electroanal. Chem*. **2000**, *493*, 28–36.
29. Rubinstein, I.; Steinberg, S.; Tor, Y.; Shanzer, A.; Sagiv, J. *Nature* **1988**, *332*, 426–429.
30. Borges, G.; Kanazawa, K.; Gordon, J. G.; Ashley, K.; Richer, J. *J. Electroanal. Chem*. **1994**, *364*, 281–284.
31. Zei, M. S.; Qiao, G.; Lehmpfuhl, G.; Kolb, D. M. *Ber. Bunsenges, Phys. Chem*. **1987**, *91*, 349–353.
32. Shi, Z.; Lipkowski, J. *J. Electroanal. Chem*. **1994**, *364*, 289–294.
33. Kondo, T.; Yanagida, M.; Shimazu, K.; Uosaki, K. *Langmuir* **1998**, *14*, 5656–5658.
34. Ishida, T.; Choi, N.; Mizutani, W.; Tokumoto, H.; Kojima, I.; Azehara, H.; Hokari, H.; Akiba, U.; Fujihira, M. *Langmuir* **1999**, *15*, 6799–6806.
35. Pressprich, K. A.; Maybury, S. G.; Thomas, R. E.; Linton, R. W.; Irene, E. A.; Murray, R. W. *J. Phys. Chem*. **1989**, *93*, 5568–5575.
36. Bard, A. J.; Faulkner, L. R. *Electrochemical Methods: Fundamentals and Applications*; 2nd edit; John Wiley & Sons, Inc.: New York, 2001.
37. Yamamoto, Y.; Nishihara, H.; Aramaki, K. *J. Electrochem. Soc*. **1993**, *140*, 436–443.

38. Randles, J. E. B. *Discussions Faraday Soc*. **1947**, *1*, 11–19.
39. Ihara, T.; Maruo, Y.; Takenaka, S.; Takagi, M. *Nucleic Acids Res*. **1996**, *24*, 4273–4280.
40. Yamana, K.; Kumamoto, S.; Hasegawa, T.; Nakano, H.; Sugie, Y. *Chem. Lett*. **2002**, 506–507.
41. Boon, E. M.; Pope, M. A.; Williams, S. D.; David, S. S.; Barton, J. K. *Biochem*. **2002**, *41*, 8464–8470.
42. Steel, A. B.; Herne, T. M.; Tarlov, M. J. *Anal. Chem*. **1998**, *70*, 4670–4677.